

Gamma Ray Bursts as Sources of Exotic Particles

Ian Morgan^a, Ted Tao^{a,*}, Erin De Pree^a, Kevin Tennyson^{a,b}

^a*Department of Physics, St. Mary's College of Maryland, St. Mary's City MD 20686*

^b*College of Earth, Ocean, and Atmospheric Sciences, Oregon State University, Corvallis, OR 97331*

Abstract

We consider the possible production of stable lightest first level KK particle (LKP) in baryonic gamma ray bursts (GRB) out flows. We numerically computed the energy-dependent cross-sections of Kaluza-Klein (KK) excitations for the Standard Model gauge bosons, γ and Z^0 . Next, we determined the feasibility of producing these KK excitations in gamma-ray emitting regions of GRBs. We found that a GRB fireball that accelerates baryons to energies greater than 10^{14} eV could produce KK excitations out to approximately 10^{12} cm from the central engine, indicating that GRBs may be a significant source of the LKP. Finally, we explore the potential observational consequences of our results.

Keywords: gamma-ray burst, kaluza-klein, dark matter candidate

1. Introduction

Kaluza-Klein (KK) theory allows all standard model (SM) fields to propagate into compact extra dimensions [1], which is a simple extra-dimensional extension of the SM with a dark matter candidate. All fields are assumed to propagate in a flat space-time $\mathcal{M}_4 \times \mathcal{S}_1$ where \mathcal{S}_1 is the extra dimension compactified on a circle. Since the fields are confined and must be continuous, a discrete series of particles arises. The momentum of the particles in the extra dimension appears as part of the apparent 4D mass. This creates a tower of KK resonances (or excitations) for each particle. Each excitation

*Corresponding author

Email addresses: ilmorgan@smcm.edu (Ian Morgan), ttao@smcm.edu (Ted Tao), ekdepree@smcm.edu (Erin De Pree)

is heavier than the last and has the same quantum numbers and spin as the 4D particle.

The mass of the n th mode in the KK tower, m^n , is given by,

$$(m^n)^2 = \left(\frac{n}{R}\right)^2 + (m^0)^2. \quad (1)$$

where m^0 is the mass of the 4D particle (also called the zeroth order KK mode) and R is the radius of the compactified extra dimension.

The momentum conservation in the extra dimensions leads to the conservation of KK number at each vertex. Conservation of KK parity requires that interactions only occur between even-number or odd-number KK modes. Thus, there exists a lightest first level KK particle (LKP), usually a linear combination the KK photon and the KK with suppressed decay cross section to the SM zero modes [2]. The unstable KK modes will quickly decay into the SM zero mode or the stable LKP. The identity of the LKP crucially depends on the mass spectrum of the first KK mode. Moreover, the LKP is considered a promising dark matter candidate because it is long-lived and has low annihilation cross sections [3]. The current Large Hadron Collider (LHC) limit on the compactification scale is $R^{-1} \geq 715$ GeV and the mass of the LKP $M_{KK} \geq 1.4$ TeV [4].

Experimentally, direct detection searches are attempt to isolate rare interactions between dark matter (DM) and ordinary matter. For example, the Large Underground Xenon (LUX) [5] and XENON-100 [6] dark matter experiments searched for events in liquid xenon target by recreating the light received by photomultipliers. These efforts are limited by a DM candidate's mass and its scattering cross-section, and their maximum possible sensitivity depends on background signal from coherent neutrino scattering.

There are also indirect methods that search for evidence of rare annihilation or scattering events elsewhere in the universe. In fact, the experimental results from numerous instruments, e.g. Fermi and PAMELA, have noted an excess in the cosmic electron-positron spectrum, which may be consistent with the annihilation events of 3 TeV DM [7, 8]. However, these findings are open to interpretation, especially since the signals cannot be localized to known DM sources [9].

On the theoretical front, recent work on indirect astrophysical detection of exotic dark matter candidates [10] explored radiation signatures from electron-dark matter scattering near active galactic nuclei, reaching the rather

pessimistic conclusion that such signals are probably undetectable with existing and near future instruments. In the more specific context of active galactic nuclei (AGN) jets, [11] performed a more detailed calculation that included specific candidate particles including the KK. They found that resonances dictated by exotic particle mass spectrum may dominate scattering between proton (or electron) and dark matter candidates, resulting in a potentially detectable break in the gamma ray spectra from AGNs. However, these studies assumed that the exotic dark matter already exist in sufficient quantities, and did not consider how such particles may have been produced.

In this work, we propose a potential astrophysical scenario for the production of the LKP as DM, and discuss the possible observational implication. DM searches that rely on rare interactions, restricts the number of events that we can observe. Particle accelerators overcome this by creating events, yet are limited by the energies that are required to create these events. However, some cosmic particle accelerators in our universe that do not have the same energy constraints, including active galactic nuclei, supernova remnants (SNR), and gamma ray bursts (GRB). The improving sensitivity of gamma-ray instruments may enable us to search for potential DM matter signatures in the gamma ray regime from such cosmic accelerators.

We show that a combination of the current theories for KK DM and GRB dynamics means that GRBs could produce KK DM in appreciable quantities. GRBs are attractive possibilities because they are, at least in principle, plausible sources for ultra-high energy cosmic rays at energies between $10^{18.5}$ to $10^{20.5}$ eV, especially if the lower energy cosmic rays can come from other systems such as supernova remnants [12, 13]. In this context, baryon-loaded GRB fireballs may accelerate protons and neutrons to above 10^{20} eV [14], possibly via a combination of first and second order Fermi acceleration [15] at shocks. Furthermore, GRBs create mildly relativistic shocks with the interstellar medium (ISM) [16]. They may also create strongly shocked regions, when fireball outflows, with randomly distributed energies, collide. Moreover, the millisecond variability of GRB light curves may rise from multiple shells ejected by the central engine, so it is possible for there to be several internal collisions. Particle encounters about these shocks generate particle showers which are translated into the gamma-rays. These particle showers may be frequent and energetic enough to produce KK excitations. Beyond high energy cosmic rays physics, these hadronic models also have garnered significant attention due to their potential to explain a range of observations [17, 18, 19]. We refer interested readers to review articles such as [20, 21, 22]

and [23] as well as further references for more details regarding the rich and fascinating phenomenology of GRBs.

We use the fireball model from [24] to estimate physical properties of the fireball. We assume a baryon-dominated fireball as such outflows are more likely to generate significant quantities of high-energy particle encounters compared to Poynting dominated scenarios. Next, we numerically compute the energy-averaged cross-section of processes involving KK particles, and combine these results with the collision region parameters to obtain an excitation rate and optical depth. These results then enable us to identify, at a qualitative level, potential signatures of the KK theory in GRBs.

Our paper is organized as follows. In Section 2.1 we outline our numerical cross-section computations and some necessary aspects of KK particle physics. Section 2.2 then explains the GRB dynamics relevant to our calculation while summarizing relevant results from [24]. Section 2.3 then explains the reaction rate calculations. In Section 3 we present our main findings. In Section 4, we discuss our results and the potential observational implications.

2. Methods

2.1. *KK excitation at high energies*

We used the computer program Pythia 8 [25] to simulate proton-proton collisions with and without a TeV^{-1} sized extra dimension [2]. We assume that any resulting KK tower quickly decays into either the LKP or SM particles. The LKP was given a set mass of 1.5 TeV, slightly above the current limits set by the LHC. These calculations are consistent with ongoing dilepton searches at the LHC [4]. To represent all the relevant interactions, we included the processes $f\bar{f} \rightarrow \sum_n (\gamma^*/Z^*)_n \rightarrow F\bar{F}$ where $f(F)$ can be any initial (final) state fermion.

The KK bosons mediate processes between fermions [26]. The KK excitation masses are dependent on the extra dimension size R through the relation $m^* \equiv R^{-1}$, where m^* is the mass of the KK excitation. Thus, for the LKP n^{th} KK excitation masses $m_{Z^*}^{(n)}$ and $m_{\gamma^*}^{(n)}$ are given by,

$$m_{Z^*}^{(n)} = \sqrt{m_{Z^*}^2 + (n \cdot m^*)^2} \quad (2)$$

$$m_{\gamma^*}^{(n)} = n \cdot m^* \quad (3)$$

We performed our calculations at logarithmically spaced energies starting from the LHC energy, 14 TeV, to the maximum astrophysical energies, $\sim 10^8$

TeV. We report the computed cross sections $\sigma(E)$ in figure 3 where E is the beam energy. A larger cross section indicates a higher probability that fermionic processes will be mediated by a KK boson. All simulated values were for a 95% confidence interval.

2.2. GRB Dynamics

The excitation rate per unit volume is a Lorentz-invariant quantity and is dependent on the cross section for KK excitation and the number and energy of the protons in the outflow. In GRBs, for these KK excitations to be appreciable, they must proceed quickly with respect to the time-scales of the bursts. The gamma-ray flux from GRBs may last anywhere from two to several hundreds of seconds, with a few notable exceptions [27]. In the previous section, we calculated the probability that a collision will give a KK excitation. In this section, we describe the energy distribution of protons in the outflow.

In our model, the central engine is spherical and its mass is concentrated in baryons. Since GRBs preferentially occur in areas with low metallicity [28], we assume a flow composed of free neutrons and protons. For long GRBs, the progenitor object is believed to be a massive star collapsing into a blackhole, so that the initial size is on the order of the Schwarzschild radius $R_0 \gtrsim 2GM_0/c^2 \sim 10^3 - 10^5$ m. The energy of the burst is related to its mass by $M_0 = E_0/\Gamma c^2$, where isotropic energy output of a GRB can reach up to 10^{54} ergs [29]. The energy imparted to this mass $M_0 \ll E_0/c^2$, within the initial radius R_0 , forces a relativistic expansion of the material. The relativistic outflows of GRBs have a coasting Lorentz factor on the order of $\Gamma_0 \gtrsim 100 - 1000$. An average coasting Lorentz factor of 100 and an isotropic energy output of 10^{54} ergs would suggest an outflow mass with $M_0 \sim 10^{-3}M_\odot$. The coasting Lorentz factor is reached at a saturation radius R_s . The Lorentz factor as a function of distance from the central engine R is therefore

$$\Gamma(r) = \begin{cases} R/R_0 & \text{if } R \leq R_{sat} \\ \Gamma_0 & \text{if } R \geq R_{sat} \end{cases}, \quad (4)$$

where saturation radius is defined by $R_s \simeq r_0\Gamma_0$.

As the fireball expands into a relativistic outflow, the initial thermal energy of the fireball is progressively converted to kinetic energy. From the observers frame, the outflow organizes into a radial shell of width $\Delta R \sim R_0$ with the mass of the outflow given by $M = Nm_b$, where N is the number of baryons and m_b is the baryon mass. We assume that protons and neutron

have approximately the same mass, hence $m_b \approx m_p$. The comoving proton density is given by,

$$n'_p \approx \frac{E_0 x}{4/3\pi R_0^3 c^2 m_b \Gamma} \quad (5)$$

where x is the proton fraction, i.e. $x = n_p/n_b$, which we assume to be 0.5.

As the relativistic outflow expands into the ISM, it produces shocks which inject baryons from the ISM into the shell. GRBs generally occur in dense star forming regions, therefore we assume that the ISM has a number density of $n_{ISM} = 1 \text{ cm}^{-3}$. The shell will continue to propagate with Lorentz factor Γ_0 in the coasting phase until it reaches the spreading phase at r_S . In the spreading phase, the shell expands with its local sound speed due to the velocity difference within the shell. The shell continues to propagate and expand, reaching the deceleration radius r_D , it begins to lose kinetic energy to the cold ISM. At which point,

$$r_D = \frac{3E_0}{4\pi n_{ISM} m_b c^2 \Gamma_0^2}. \quad (6)$$

Internal collisions occur when a shell catches up to another shell. Consider a system where each of the shells ejected from the central object have random mass-energy injections and dimensionless velocity β , where $\Gamma = 1/\sqrt{1-\beta^2}$. This phenomenon produces a number of internal collisions between these shells.

Consider a faster shell ejected sometime after a slower shell, ΔT . The faster shell, henceforth denoted by the subscript f , will sweep into the slower shell, henceforth denoted by the subscript s . The faster shell injects energy into the slower shell, thus it will be called the injective shell. The slower shell receives the injection of energy in the form of baryons. The collision creates a shock between the two shells, similar to the shock created between the shell and the ISM. The radius at which these two shells collide is

$$r_{coll} \simeq 2\Gamma_s^2 c(\Delta T)/(1 - \Gamma_s/\Gamma_f), \quad (7)$$

where Γ_f and Γ_s are the Lorentz factors of the fast and slow shell respectively. Notice that in the limiting case where $\Gamma_f \gg \Gamma_s$ that this reduces to $r_{coll} \simeq 2\Gamma_s^2(c\Delta T)$. For a shells with $\Gamma_f = 300$ and $\Gamma_s = 1$, $r_{coll} \sim 10^6 \text{ m}$ if the fast shell is ejected 10 ms after the slow shell.

2.3. Excitation Rate and Optical Depth

KK excitation may occur in shocked regions as the outflow collides with either the ISM or a slower shell. The shocks facilitate diffusive and stochastic acceleration of the baryons, which results in a power-law energy distribution $n_p(E) \propto (E/E_0)^{-\alpha}$, where the spectral index is $\alpha \approx 2$. We take the width of the shocked region to be $\Delta R \sim R_0$.

Once the protons have been accelerated above the resonant energy, collisions may produce KK excitations. To quantify the importance of KK-mediated processes, we compute an excitation optical depth

$$\tau_{KK} \approx \frac{n_b(r) \langle \sigma_{KK}(r) \rangle \Delta R}{\Gamma} \quad (8)$$

as a function the distance r where the shell smashes into either a slower shell or the ISM. Here we take the region where significant KK mediated collisions occur to be about the shell width ΔR , and n_b is the baryon number density in this region that depends on both r and the nature of the medium that the shell runs into. To compute τ_{KK} , we use a energy-averaged cross section

$$\langle \sigma_{KK}(r) \rangle = \frac{\int \sigma(E, r) \phi(E, r) dE}{\int \phi(E, r) dE}, \quad (9)$$

where $\phi(E, r) = n_b(E, r)v \approx n_b(E, r)c$ is the energy-dependent proton flux in the highly relativistic flow. Here we assumed that $n_b(E, r)$ is approximately spatially constant across ΔR . We report τ_{KK} in figure 3 for different scenarios.

Finally, we calculate the production rate. The nuclear collision rate is given by, $\dot{n}_{coll}(E) = n_{p,1}(E)\sigma(E)n_{p,2}c/\Gamma_{rel}$. The protons in $n_{p,2}$ are assumed to be stationary with respect to $n_{p,1}(E)$. This assumption is intuitive for shocks with the ISM. While injections of protons by the ISM may be accelerated in these shocks, it is much more reasonable that they collide with the already accelerated protons. Thus, the production rate is $\dot{n}_{KK}(E) = n_{p,s}(E)\sigma(E)n_{p,ISM}c/\Gamma_{rel}$, where $n_{p,s}$ and $n_{p,ISM}$ are the particle densities for the shell and ISM, respectively. In internal collisions, the assumption is that there is a fast shell and a slow shell. In the strongly shocked internal collision region, there may be head-on and tail collisions. In the dynamics of Fermi acceleration, head-on collisions are much more likely [16]. If $\Gamma_{rel} \gg 1$, then this simplifies to collisions with a stationary target. Thus, $\dot{n}_{KK}(E) = n_{p,f}(E)\sigma(E)n_{p,s}c/\Gamma_{rel}$, where $n_{p,f}$ and $n_{p,s}$ are the particle densities for the fast and slow shell, respectively.

3. Results

Our calculation gives the number of events as a function of energy, and a total cross section. As the collision energy rises, the KK excitation cross section increases and diverges further from its SM counterpart due to the larger influence from higher order processes [30]. The cross section for producing quark antiquark pairs is approximately an order of magnitude greater than for producing leptons. All cross sections are within a 95% confidence interval. These Monte Carlo generated cross sections are shown in figure 3.

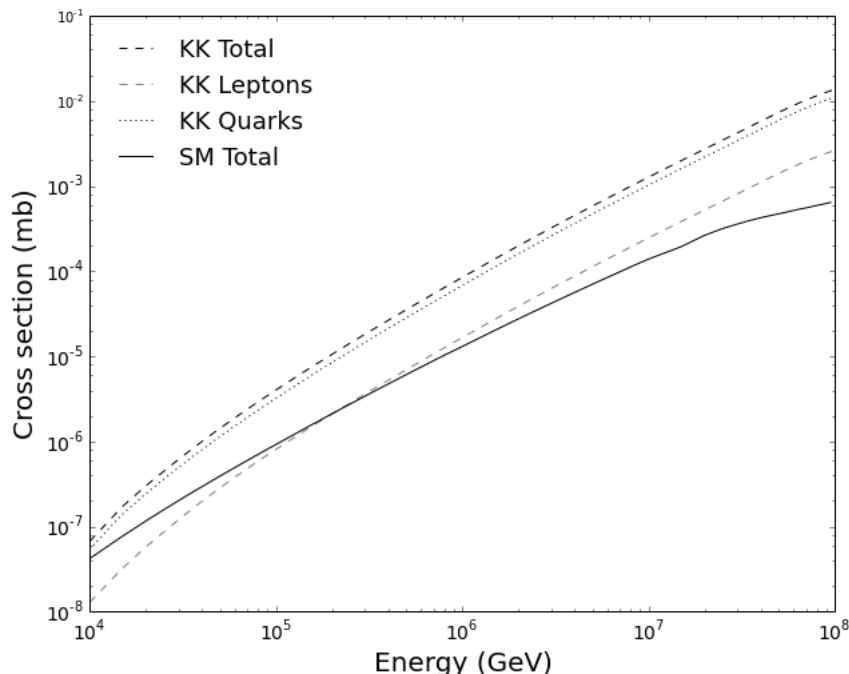


Figure 1: Pythia8 generated cross sections for KK excitations. All values are within a 95% confidence interval.

We calculated production rates when a shell smashes into the ISM, a dense molecular cloud, and a slower shell. For the shells, we used a mass of $10^{-3} M_{\odot}$, which is consistent with the mass estimates in section 2.2. We assumed that Fermi-type acceleration generated a power-law spectrum for the differential particle densities in the shocks with energies from 100 to 10^8 GeV and a Lorentz factor of 300. For the internal collisions, we report the reaction rates between two shells with the same mass, a fast shell with

a Lorentz factor of 300, and a slower target shell with a Lorentz factor of 1. The KK excitation rates are reported in figure 3. The total reaction rates in $\text{cm}^{-3}\text{s}^{-1}$ were 53, 5300, and 5.3×10^{33} for ISM case, dense cloud case, and internal collisions.

4. Conclusions and Observational Implications

Our results indicate that KK excitations could be significant as a GRB fireball shell collides with another medium, especially since KK mediated processes enjoy vastly boosted cross-sections over their SM equivalents over the relevant energy range. In particular, we found that collisions with the ISM and a dense cloud would produce KK excitations, but at a much slower rate than internal collisions. Despite the increase in the cross-section with particle energy, the excitation rate decreases as there are fewer protons at higher energies.

Reference [2] found a characteristic peak and valley in the KK excitation rate as a function of beam energy. The suppression and boosting of the cross section that leads to these features is consistent with our simulations. The LKP should be identifiable by the characteristic suppression of the number of events near its resonant rest mass energy (1.59 TeV in our work). This would in turn lead to a decrease in gamma ray output from a GRB near and above this energy scale. Such a dark matter production signal does not conflict with any observational constraints, and would account for the signals gamma-ray excess from the Fermi and Pamela experiments. In the near future, improvements to the current generation of TeV instruments, the newly operational High-Altitude Water Cherenkov Observatory (HAWC) experiment, and the planned Cherenkov Telescope Array (CTA) experiment aim to observe GRBs in the TeV regime. In particular, CTA is expected to revolutionize the study of cosmic particle accelerators, and may provide further evidence of DM production.

We assumed that GRB fireballs are baryon dominated, however other theories assume that the outflow is composed of leptons, primarily electrons. The resulting spectrum is then from one of or a combination of synchrotron, inverse Compton, and synchrotron self-Compton. The benefits of these leptonic models include their relative simplicity, and the numerous adjustable parameters for fitting purposes. On the other hand, the complexity of hadronic models has limited their use in simulations as the codes must keep track of all the particles from particle showers and determine their contribution to

the spectrum. Despite these difficulties, there has been some recent work attempting to explain observations with hadronic flows [18, 31]. Using similar methods, we hope to compute the predicted GRB spectrum taking KK excitations into account.

In the future, we also intend to explore the possibility that SNR may be significant KK production environments. As a source of galactic cosmic rays, SNRs also create shocks and accelerate protons. SNRs live longer than GRBs and have been observed in the TeV range [32]. Furthermore, hadronic, photopion models have already been shown to fit the gamma-ray spectrum from SNRs [33].

5. Acknowledgements

The authors acknowledge the support from St. Mary's College of Maryland faculty development grant. We also appreciate insightful discussions with P. Meszaros and O. Blaes.

References

References

- [1] A. Salam, J. Strathdee, On Kaluza-Klein Theory, *Annals Phys.* 141 (1982) 316–352. doi:10.1016/0003-4916(82)90291-3.
- [2] G. Bella, E. Etzion, N. Hod, Y. Oz, Y. Silver, et al., A Search for heavy Kaluza-Klein electroweak gauge bosons at the LHC, *JHEP* 1009 (2010) 025. arXiv:1004.2432, doi:10.1007/JHEP09(2010)025.
- [3] G. Servant, T. M. Tait, Is the lightest Kaluza-Klein particle a viable dark matter candidate?, *Nucl.Phys. B* 650 (2003) 391–419. arXiv:hep-ph/0206071, doi:10.1016/S0550-3213(02)01012-X.
- [4] L. Edelhuser, T. Flacke, M. Krmer, Constraints on models with universal extra dimensions from dilepton searches at the LHC, *JHEP* 1308 (2013) 091. arXiv:1302.6076, doi:10.1007/JHEP08(2013)091.
- [5] D. Akerib, X. Bai, S. Bedikian, E. Bernard, A. Bernstein, et al., Data Acquisition and Readout System for the LUX Dark Matter Experiment, *Nucl.Instrum.Meth. A* 668 (2012) 1–8. arXiv:1108.1836, doi:10.1016/j.nima.2011.11.063.

- [6] E. Aprile, et al., The XENON100 Dark Matter Experiment, *Astropart.Phys.* 35 (2012) 573–590. [arXiv:1107.2155](#), [doi:10.1016/j.astropartphys.2012.01.003](#).
- [7] D. Grasso, et al., On possible interpretations of the high energy electron-positron spectrum measured by the Fermi Large Area Telescope, *Astropart.Phys.* 32 (2009) 140–151. [arXiv:0905.0636](#), [doi:10.1016/j.astropartphys.2009.07.003](#).
- [8] M. Boezio, M. Pearce, P. Picozza, R. Sparvoli, P. Spillantini, et al., PAMELA and indirect dark matter searches, *New J.Phys.* 11 (2009) 105023. [doi:10.1088/1367-2630/11/10/105023](#).
- [9] A. Taylor, J. Hinton, P. Blasi, M. Ave, Identifying Nearby UHECR Accelerators using UHE (and VHE) Photons, *Phys.Rev.Lett.* 103 (2009) 051102. [arXiv:0904.3903](#), [doi:10.1103/PhysRevLett.103.051102](#).
- [10] E. D. Bloom, J. D. Wells, Multi - GeV photons from electron - dark matter scattering near active galactic nuclei, *Phys.Rev.* D57 (1998) 1299–1302. [arXiv:astro-ph/9706085](#), [doi:10.1103/PhysRevD.57.1299](#).
- [11] M. Gorchtein, S. Profumo, L. Ubbaldi, Probing Dark Matter with AGN Jets, *Phys.Rev.* D82 (2010) 083514. [arXiv:1008.2230](#), [doi:10.1103/PhysRevD.84.069903](#), [doi:10.1103/PhysRevD.82.083514](#).
- [12] E. Waxman, Cosmological gamma-ray bursts and the highest energy cosmic rays, *Phys.Rev.Lett.* 75 (1995) 386–389. [arXiv:astro-ph/9505082](#), [doi:10.1103/PhysRevLett.75.386](#).
- [13] M. Vietri, On the acceleration of ultrahigh-energy cosmic rays in gamma-ray bursts, *Astrophys.J.* 453 (1995) 883–889. [arXiv:astro-ph/9506081](#), [doi:10.1086/176448](#).
- [14] E. Waxman, Gamma-ray bursts: Potential sources of ultra high energy cosmic-rays, *Nucl.Phys.Proc.Suppl.* 151 (2006) 46–53. [arXiv:astro-ph/0412554](#), [doi:10.1016/j.nuclphysbps.2005.07.008](#).
- [15] K. Murase, K. Asano, T. Terasawa, P. Meszaros, The Role of Stochastic Acceleration in the Prompt Emission of Gamma-Ray Bursts: Application to Hadronic Injection, *Astrophys.J.* 746 (2012) 164. [arXiv:1107.5575](#), [doi:10.1088/0004-637X/746/2/164](#).

- [16] E. Fermi, On the Origin of the Cosmic Radiation, *Phys.Rev.* 75 (1949) 1169–1174. doi:10.1103/PhysRev.75.1169.
- [17] K. Asano, S. Inoue, P. Meszaros, Prompt High-Energy Emission from Proton-Dominated Gamma-Ray Bursts, *Astrophys.J.* 699 (2009) 953–957. arXiv:0807.0951, doi:10.1088/0004-637X/699/2/953.
- [18] K. Asano, S. Guiriec, P. Meszaros, Hadronic Models for the Extra Spectral Component in the short GRB 090510, *Astrophys.J.* 705 (2009) L191–L194. arXiv:0909.0306, doi:10.1088/0004-637X/705/2/L191.
- [19] J. Racusin, S. Karpov, M. Sokolowski, J. Granot, X. Wu, et al., GRB 080319B: A Naked-Eye Stellar Blast from the Distant Universe, *Nature* 455 (2008) 183–188. arXiv:0805.1557, doi:10.1038/nature07270.
- [20] N. Gehrels, E. Ramirez-Ruiz, D. B. Fox, Gamma-Ray Bursts in the Swift Era, *Ann.Rev.Astron.Astrophys.* 47 (2009) 567–617. arXiv:0909.1531, doi:10.1146/annurev.astro.46.060407.145147.
- [21] N. Gehrels, S. Razzaque, Gamma Ray Bursts in the Swift-Fermi Era, *Front.Phys.China* 8 (2013) 661–678. arXiv:1301.0840, doi:10.1007/s11467-013-0282-3.
- [22] P. Meszaros, Gamma Ray Bursts, *Astropart.Phys.* 43 (2013) 134–141. arXiv:1204.1897, doi:10.1016/j.astropartphys.2012.03.009.
- [23] E. Berger, Short-Duration Gamma-Ray Bursts, *Ann.Rev.Astron.Astrophys.* 52 (2014) 43–105. arXiv:1311.2603, doi:10.1146/annurev-astro-081913-035926.
- [24] B. Zhang, P. Meszaros, Gamma-ray bursts with continuous energy injection and their afterglow signature, *Astrophys.J.* 566 (2002) 712–722. arXiv:astro-ph/0108402, doi:10.1086/338247.
- [25] T. Sjostrand, S. Mrenna, P. Z. Skands, A Brief Introduction to PYTHIA 8.1, *Comput.Phys.Commun.* 178 (2008) 852–867. arXiv:0710.3820, doi:10.1016/j.cpc.2008.01.036.
- [26] D. Dannheim, Probing Extra Dimensions with ATLAS, *AIP Conf.Proc.* 903 (2007) 261–264. arXiv:hep-ex/0611005, doi:10.1063/1.2735175.

- [27] C. Kouveliotou, C. A. Meegan, G. J. Fishman, N. P. Bhyat, M. S. Briggs, et al., Identification of two classes of gamma-ray bursts, *Astrophys.J.* 413 (1993) L101–104. doi:10.1086/186969.
- [28] S. Woosley, A. Heger, The Progenitor stars of gamma-ray bursts, *Astrophys.J.* 637 (2006) 914–921. arXiv:astro-ph/0508175, doi:10.1086/498500.
- [29] P. Meszaros, Gamma-Ray Bursts, *Rept.Prog.Phys.* 69 (2006) 2259–2322. arXiv:astro-ph/0605208, doi:10.1088/0034-4885/69/8/R01.
- [30] A. Djouadi, G. Moreau, R. K. Singh, Kaluza-Klein excitations of gauge bosons at the LHC, *Nucl.Phys. B* 797 (2008) 1–26. arXiv:0706.4191, doi:10.1016/j.nuclphysb.2007.12.024.
- [31] A. M. Beloborodov, Collisional mechanism for GRB emission, *Mon.Not.Roy.Astron.Soc.* 407 (2010) 1033. arXiv:0907.0732, doi:10.1111/j.1365-2966.2010.16770.x.
- [32] F. Aharonian, et al., HESS Observations and VLT Spectroscopy of PG 1553+113, *Astron.Astrophys.* 477 (2008) 481–489. arXiv:0710.5740, doi:10.1051/0004-6361:20078603.
- [33] M. Ackermann, et al., Detection of the Characteristic Pion-Decay Signature in Supernova Remnants, *Science* 339 (2013) 807. arXiv:1302.3307, doi:10.1126/science.1231160.

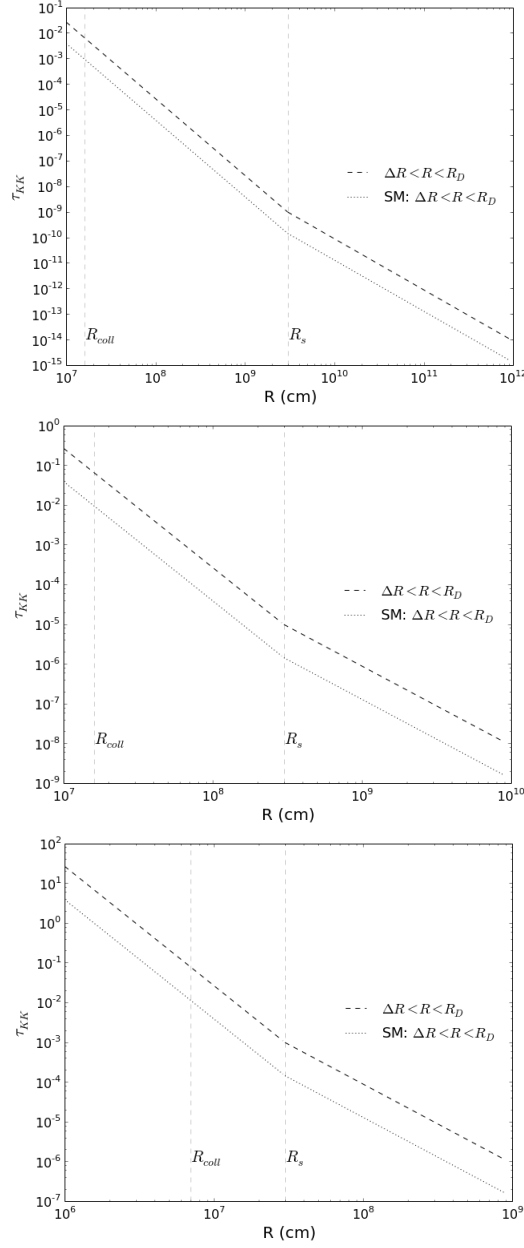


Figure 2: Energy integrated production optical depth for KK excitations for various parameters. The optical depth indicates the likelihood that a particle will undergo collisions resulting KK excitation while traveling across the width of a shell. The plot is a function of the distance between the shell and the central engine. In the case of a purely SM regime, this is equivalent to the production optical depth SM bosons γ or Z^0 . The shell density is 10^{33} cm^{-3} with a energy distribution that follows a power law with index $\alpha = -2$. The width of the shell is 10^7 cm . The Lorentz factor is 300. In the upper left panel, we assume multiple shells expanding with particle density n_0 on the order of 10^{33} cm^{-3} . The upper right panel assume that the shell has slowed and the Lorentz factor is 30. Finally, the lower panel assume that the burst outputs a single shell with 10^{35} cm^{-3} and Lorentz factor is 30.

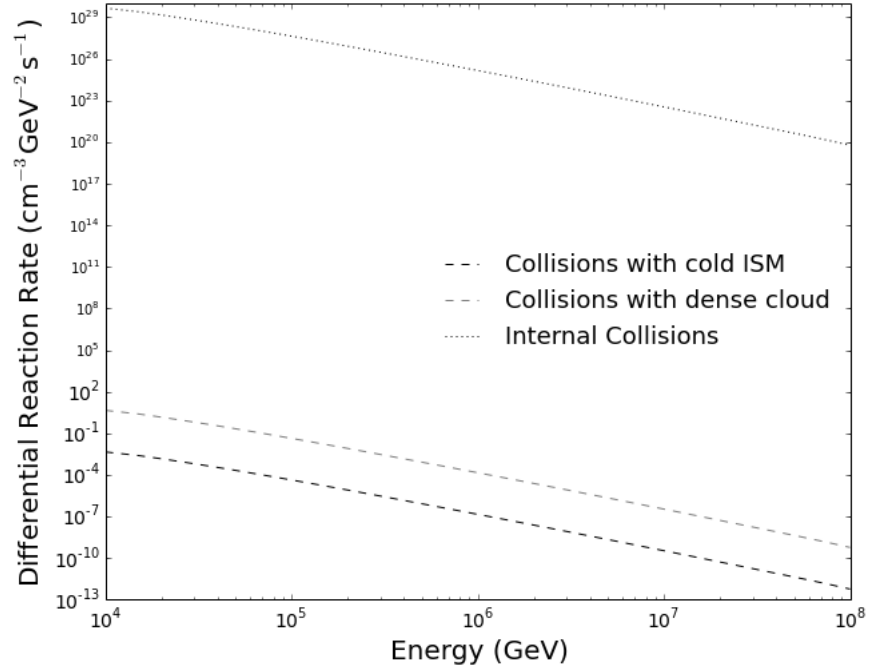


Figure 3: Differential reaction rate for KK excitations. The densities are 1 cm^{-3} and 1000 cm^{-3} for the ISM and dense molecular cloud, respectively. The isotropic energy output for the baryons associated with each shell is 10^{52} ergs and the initial radius is 10^7 cm. The incident particle density n_0 was on the order of 10^{33} cm^{-3} . For internal collisions, we assume that the slow shell has slowed such that $\Gamma_{rel} \sim \Gamma_f$.